Journal of Thermal Analysis and Calorimetry (2021) 145:609–630
https://doi.org/10.1007/s10973-020-09756-y

ANN modelling and experimental investigation on effective thermal conductivity of ethylene glycol:water nanofluids

K. Marigowda Yashawantha[1] · A. Venu Vinod[1]

Received: 12 December 2019 / Accepted: 27 April 2020 / Published online: 13 May 2020

Abstract

In this study, ethylene glycol (EG)–water (35:65 %v)-based nanofluids have been prepared to study enhancement in thermal conductivity. Nanofluids containing nanoparticles of materials CuO, Al_2O_3 and TiO_2 of different mass concentrations from 0.2 to 2% were prepared using ultrasonication. Thermal conductivity measurement was carried using KD2 Pro thermal properties analyser in the temperature range of 30–60 °C. The study investigated the effect of concentration of nanoparticles, temperature and nanoparticle material on effective thermal conductivity of nanofluids. The results showed a significant improvement in effective thermal conductivity due to the addition of nanoparticles to the base fluid. Correlations were developed for predicting the effective thermal conductivity considering each material separately, and a generalized correlation considering the three materials. Subsequently, ANN modelling was carried out for predicting the effective thermal conductivity of nanofluids and compared with developed correlations. The modelling work carried out in this study is more generalized as literature results were considered in addition to the results from the present study. ANN modelling predicts the effective thermal conductivity better than the proposed correlations.

Keywords Nanofluids · Effective thermal conductivity · EG:water mixture · Nanoparticles · ANN modelling

List of symbols

C_p	Specific heat (kJ kg^{-1} K)
k	Thermal conductivity (W m^{-1} K^{-1})
T	Temperature (K)
m	Mass of nanoparticles
cP	Centi poise

Abbreviations

EG:W	Ethylene glycol and water mixture
DI	Distilled water
ANN	Artificial neural network
FF	Feed forwards
MAD	Mean average deviation
MSE	Mean square error
MAPE	Mean absolute percentage error
ASHRAE	American Society for Heating Ventilation and Air-Conditioning Engineers

Greek symbols

ρ	Density (kg m^{-3})
μ	Viscosity (cP)
ϕ_m	Mass fraction
$\emptyset_v$	Volume fraction

Subscripts

nf	Nanofluid
eff	Effective
bf	Base fluid
np	Nanoparticles

Introduction

Nanofluids have superior thermal conducting properties due to the presence of nanoparticles (size < 100 nm) in a base fluid. Ethylene glycol (EG), water, engine oil, propylene glycol (PEG), refrigerants etc., have been used as the base fluid to prepare the nanofluid [1–4]. Due to the small size of nanoparticles, the homogeneous distribution of nanoparticles in the base fluid can be obtained. The significance of nanofluids utilization in heat transfer has attracted many researchers. With the present advances in nanotechnology, the preparation of nanoparticles can be accomplished easily

✉ A. Venu Vinod
avv@nitw.ac.in

[1] Department of Chemical Engineering, National Institute of Technology Warangal, Warangal, Telangana 506004, India

by various methods [5]. As a result, the possibility of adding nanoparticles in a commonly used base fluid for improving thermophysical properties has been experimentally exploited by various researchers [6–10]. Thermal conductivity of the fluid is the most important property for heat transfer studies. It is also known that the larger surface area of the particles results in enhanced thermal conductivity in the base fluid. Nanoparticles of metals, metal oxides, non-metals and non-metal oxides have been used to study the thermal properties and applications in heat exchangers [11–13]. Various nanofluids have been used to carry out the studies on heat exchangers such as double pipe heat exchanger [14], shell and tube heat exchanger [15–17], helical coil heat exchanger [18, 19], plate heat exchanger [20, 21] etc.

Eastman et al. [22] used water and HE 200 oil as a base fluid to disperse the Al_2O_3, CuO and Cu nanoparticles and found thermal conductivity enhancement of 60% for the volume concentration of 5%. Further studies were carried out using EG as base fluid using Cu particles (with less than 10 nm of size) and reported 40% of enhancement for 0.3% of volume fraction [23]. Yu et al. [24] investigated the thermal conductivity of ZnO nanoparticles dispersed in EG. Results showed that thermal conductivity was strongly dependent on particle concentration and temperature.

Ethylene glycol and water (EG:W) mixture gained a lot of attention due to its low freezing point and high boiling temperature compared to water. EG:W-based nanofluids have attracted studies for applications such as car radiator, heat exchangers, chillers etc. [25]. Vajja and Das [26] reported a significant improvement in thermal conductivity for EG:W-based Al_2O_3 and CuO nanofluids. Their studies reported 69% of enhancement for 6% volume concentration of CuO nanoparticles and 10% of volume concentration for Al_2O_3 nanoparticles in EG:W base fluid. Kole and Dey [27] have carried out the thermal conductivity measurement on graphene oxide nanoparticles dispersed in a mixture of EG and DI water (70:30 v/v). Thermal conductivity was measured with varying the graphene oxide concentration (0.041–0.395 vol%) and temperature (10–70 °C). An enhancement of 15% for adding only 0.395 vol% of graphene oxide was observed at room temperature. Reddy et al. [28] performed thermal conductivity study of TiO_2 nanoparticles dispersed in EG:W (40:60) and reported an enhancement of 5% at 70 °C for 1% of volume concentration. Sundar et al. [29] prepared EG:W (50:50)-based Al_2O_3 and CuO nanofluid and examined thermal conductivity at different temperatures. Both the nanofluids were found to have enhanced thermal conductivity with respect to concentration and temperature compared with the base fluid of EG:W. However, enhancement of EG:W–CuO nanofluid was higher compared to EG:W–Al_2O_3 nanofluids. They extended their studies further for different ratios of EG:W (20:80%, 40:60% and 60:40% in mass) to study the effect of EG:W ratio, concentration of Al_2O_3 nanoparticles and temperature [30]. Maximum enhancement of 32.26% was obtained for a 20:80 ratio of EG:W at 1.5% concentration. Serebryakov et al. [31] used 90% of EG and 10% of water with Al_2O_3 nanoparticles to measure the thermal conductivity. Thermal conductivity of SiO_2 nanoparticles in EG:W (at different volume ratios) was investigated for a mass concentration of 0.3% nanoparticles with a temperature range of (25–45 °C) [32]. Thermal conductivity of EG:W–SiO_2 nanofluids decreased with the increase in EG content. Researchers have performed experimental investigations using oxides of metals such as alumina

Table 1 Thermal conductivity enhancement reported in the literature for different ratios of EG and water mixture

References	Nanoparticles/particle size	EG:water ratio	Nanoparticle vol%	Temperature/°C	Enhancement (%) in *k*
Reddy et al. [28]	TiO_2/21 nm	40:60	0.2–1	30–70	4.38–5
Sundar et al. [29]	CuO/27 nm	50:50	0.2–0.8	15–50	15.6–24.56 (0.8% vol)
	Al_2O_3/36.5 nm				9.8–17.89 (0.8% vol)
Elias et al. [33]	Al_2O_3/13 nm	50:50	0–1	10–50	8.3–9.8 (1% vol)
Sundar et al. [30]	Al_2O_3/36.5 nm	20:80	0.3–1.5	20–60	17.47–32.26 (1.5% vol)
		40:60	0.3–1.5		14.60–30.51 (1.5% vol)
		60:40	0.3–1.5		11.07–27.42 (1.5% vol)
Hamid et al. [34]	TiO_2/50 nm	40:60	0.5–1.5	30–80	7–15.35 (1.5% vol)
Chiam et al. [35]	Al_2O_3/53 nm	40:60	0.2–1	30–70	4.2–8 (1% vol)
		50:50	0.2–1		5–12 (1% vol)
		60:40	0.2–1		8–17 (1% vol)
Krishnakumar et al. [36]	TiO_2/40 nm	60:40	0.2–0.8	20–50	8–24 (0.8% vol)

Table 2 Correlations proposed for the effective thermal conductivity of nanofluids from the literature

References	Correlation	Remarks
Maxwell [37]	$k_{\text{eff}} = \frac{2k_{\text{bf}}+k_{\text{np}}+2(k_{\text{np}}-k_{\text{bf}})\emptyset_{\text{v}}}{2k_{\text{bf}}+k_{\text{np}}-(k_{\text{np}}-k_{\text{bf}})\emptyset_{\text{v}}}$	All nanofluids
Hamilton and Crosser [38]	$k_{\text{eff}} = \frac{k_{\text{np}}+k_{\text{bf}}(n-1)-(k_{\text{bf}}-k_{\text{np}})(n-1)\emptyset_{\text{v}}}{k_{\text{np}}+k_{\text{bf}}(n-1)+(k_{\text{np}}-k_{\text{bf}})\emptyset_{\text{v}}}$	Spherical and non-spherical particles. $n=3$ for spherical particles
Lu and Lin [39]	$k_{\text{eff}} = \left(\frac{k_{\text{np}}}{k_{\text{bf}}}\right)\emptyset_{\text{v}} + b\emptyset_{\text{v}}^2$	$b=2$ for spherical particles
Bhattacharya [40]	$k_{\text{eff}} = \left(\frac{k_{\text{np}}}{k_{\text{bf}}}\right)\emptyset_{\text{v}} + (1-\emptyset_{\text{v}})$	Spherical particles
Reddy et al. [28]	$k_{\text{eff}} = a + b\emptyset_{\text{v}}$ a, b and c are obtained from regression $\emptyset_{\text{v}}=0.2$–1% $T=30$–70 °C	For EG:W (40:60) mixture-based TiO_2-based nanofluids
Sundar et al. [29]	$k_{\text{eff}} = 1.262\left[\frac{T_{\max}}{T_{\min}}\right]^{-0.09214}\emptyset^{0.07379}$ $\emptyset_{\text{v}}=0.2$–0.8% $T=15$–50 °C	For EG:W (50:50) mixture-based CuO nanofluids
Sundar et al. [30]	$k_{\text{eff}} = 1.0806 + 10.164\emptyset_{\text{v}}$ $\emptyset_{\text{v}}=0.3$–1.5% $T=20$–60 °C	For EG:W (40:60) mixture-based Al_2O_3 nanofluids
Hamid et al. [34]	$k_{\text{eff}} = \left(1+\frac{\emptyset_{\text{v}}}{100}\right)^7\left(\frac{T}{80}\right)^{0.024}$ $\emptyset_{\text{v}}=0.2$–1% $T=30$–70 °C	For EG:water (60:40) mixture-based TiO_2-based nanofluids
Chiam et al. [35]	$k_{\text{eff}} = 0.9683\left(1+\frac{\emptyset_{\text{v}}}{100}\right)^{11.13}\left(1+\frac{T}{70}\right)^{0.1676}(1+BR)^{0.00111}\left(\frac{d_{\text{p}}}{36}\right)^{0.0572}$ BR—base ratio of EG water mixture(0.4–0.6) $\emptyset_{\text{v}}=0$–1.5% $T=20$–70 °C	For Al_2O_3 nanofluids of EG:water mixture
Srinivas and Vinod [1]	$k_{\text{eff}} = a(\emptyset_{\text{v}})^{\text{b}}\left(\frac{T_{\text{nf}}}{T_0}\right)^{\text{c}}\left(\frac{d_{\text{bf}}}{d_{\text{np}}}\right)^{\text{d}}$ Constants a, b and c are obtained from regression method $\emptyset_{\text{w}}=0.3$–2 mass% $T=30$–70 °C	For water-based nanofluids
Naik and Vinod [2]	$k_{\text{eff}} = a\left(\frac{T_{\text{nf}}}{T_{\text{r}}}\right)^{\text{b}}\left(\frac{\emptyset_{\text{nf}}}{\emptyset_{\text{bf}}}\right)^{\text{c}}$ a, b c and d are regression constants from experimental data $\emptyset_{\text{nf}}=0$–1 mass% $T=30$–50 °C	For CMC–water-based nanofluids

(Al_2O_3), copper oxide (CuO) and titanium oxide (TiO_2) as they are cheaper compared to the corresponding metal nanopowder. All the literature reports have shown enhancement in the thermal conductivity by the addition of nanoparticles. Table 1 summarizes the literature work reported on maximum enhancement in thermal conductivity.

Table 2 presents mathematical models for thermal conductivity for various nanofluids. The developed models such as Maxwell and Hamilton–Crosser consider basic mixture of solid particles in liquid. Some of the correlations developed in the literature are based on their experimental results as a function of temperature and concentration. However, the

development of empirical model using regression method for prediction with a multiple input variables is a difficult task due to large deviation in prediction. To overcome this disadvantage, artificial neural network (ANN) modelling can be employed for accurate prediction with several input parameters. Many researchers have performed the prediction of effective thermal conductivity (k_{nf}/k_{bf}) using ANN modelling considering the factors such as the concentration of nanofluid, temperature, particle size, etc. Hojjat et al. [41] performed ANN modelling to predict thermal conductivity for 0.5 mass% CMC-based Al_2O_3, CuO and TiO_2 nanofluids using feedforward artificial neural network (FF-ANN) considering concentration, temperature and thermal conductivity of nanoparticles as input variables. The prediction has shown good agreement with experimental results. Ariana et al. [42] carried out ANN modelling to predict the thermal conductivity of water-based Al_2O_3 nanofluids. Thermal conductivity data for various particle sizes of Al_2O_3 were collected at different concentrations and temperatures. They used FF-ANN model of two hidden layers having 14 neurons to predict the data and results showed satisfactory prediction with a regression coefficient (R^2) of 0.971, absolute average relative deviation (AARD %) of 1.27%, and mean square error (MSE) of 4.73×10^{-4}. Esfe et al. [43] developed an empirical correlation and carried out FF-ANN modelling to predict the thermal conductivity of water-based Al_2O_3 nanofluid. The correlation and ANN modelling performed well in predicting the thermal conductivity of nanofluid. One more study was carried out by them, in which ANN modelling proved better than correlation for water/EG mixture (60:40)-based MgO nanofluids [44].

Tahani et al. [45] performed ANN modelling for thermal conductivity of deionized water-based graphite oxide nanoplatelets considering mass concentration and temperature as input variables. In their study, two hidden layers with eight neurons were used to predict the thermal conductivity. From the predicted data, root mean square error (RMSE), mean absolute percentage error and R^2 were determined to evaluate the performance of ANN. Results showed the accurate prediction of the thermal conductivity with experimental data. Ahmadloo and Azizi [46] conducted ANN modelling using several inputs to predict the effective thermal conductivity of nanofluids. Similar work considering EG-based metals and metal oxides nanofluids was reported by Wang et al. [47]. Their results have shown that ANN modelling tool can be used to predict the effective thermal conductivity with minimum deviation. Esfe et al. [48] developed ANN modelling to predict the effective thermal conductivity for EG-based MgO nanofluids using experimental data and results obtained by modelling are in good agreement with the measured data. Zhao et al. [49] adopted radial basis function (RBF)-ANN approach to predict the thermal conductivity of water-based Al_2O_3 nanofluids considering concentration and temperature as an input variables. Their results concluded that ANN modelling can be used as an effective method to predict the thermophysical properties of nanofluids with an error of $\pm 2\%$. Esfe [50] developed RBF-ANN modelling to predict the thermal conductivity EG-based TiO_2 nanofluids. The results showed better than the correlation approach.

From the literature, it can be observed that there are studies reported on thermal conductivity of EG:water-based nanofluids, considering nanoparticles of CuO, Al_2O_3 and TiO_2 at lower concentration ($<0.5\%$ volume concentration). Table 1 gives an account of studies. Lower concentration of nanoparticles can provide a limited enhancement in thermal conductivity. On the other hand, due to high concentration higher viscosity of nanofluids was reported. However, the effective use of nanofluids in the applications such as heat exchangers can deliver significant improvement in heat transfer. As observed from the literature review, there have been a number of experimental and modelling studies on

Table 3 ASHRAE data for 35:65 EG:water mixture at different temperatures [51]

Temperature/°C	Density(ρ)/kg m^{-3}	Specific heat (C_p)/kJ kg^{-1}	Thermal conductivity (k)/W m^{-1} K^{-1}	Viscosity (μ)/cP
25	1050.46	3.5725	0.429	2.245
30	1048.325	3.588	0.4335	1.975
35	1046.435	3.603	0.437	1.745
40	1043.7	3.6185	0.441	1.56
45	1041.205	3.634	0.4445	1.4
50	1038.58	3.6495	0.448	1.26
55	1035.845	3.665	0.4505	1.14
60	1032.985	3.833	0.4535	1.035

Table 4 Details of nanoparticles used in the present study

	CuO (Alfa Aeasar)	Al_2O_3 (Alfa Aesar)	TiO_2 (Rutile) (Nanoshell USA)
APS	30–50 nm	40–50 nm	40–45 nm
Purity	99%	99.5%	99.9%
Molecular mass	79.55 g mol^{-1}	101.96 g mol^{-1}	79.866 g mol^{-1}
Colour	Black	White	White
True density	6.3 g cc^{-1}	3.97 g cc^{-1}	3.9 g cc^{-1}
Melting point	1326 °C	2045 °C	1843 °C
SSA	13 m^2 g^{-1}	32-40 m^2 g^{-1}	>30 m^2 g^{-1}

EG:W mixture using various nanopowders. However, it can be seen that the modelling work pertained only to the respective experimental studies. No generalized models have been reported. In this work, a generalized correlation and ANN model have been developed to predict the effective thermal conductivity of nanofluids using the experimental results (35:65 (V/V)) from the present study and literature data for EG:W-based nanofluids.

Materials and methods

Preparation of nanofluid

The mixture of ethylene glycol and water 35:65 (volume/volume) was used as base fluid in the present study. Table 3 shows the thermophysical properties of EG:W from ASHRAE [51]. Nanoparticles of CuO, Al_2O_3 and TiO_2 were used to prepare the EG:W-based nanofluids separately. Table 4 shows the details of the nanopowders.

The required amount of nanopowder for preparing nanofluids of mass concentration of 0.2%, 0.5%, 1%, 1.5% and 2% is calculated using Eq. (1).

$$100\,\emptyset_m = \frac{m_g}{m_g + m_{EG/w}} \tag{1}$$

where m_g $m_{EG/w}$ = mass of graphite nanoparticles and base fluid, respectively. $\emptyset_m$ = Mass fraction of nanopowder.

Before adding the nanoparticles to 40 mL of the base fluid, 0.2% mass concentration of sodium dodecyl benzene sulphonate (SDBS) surfactant was added to base fluid and stirred to maintain a stable dispersion and to provide long-term stabilization of nanofluid. The required amount of nanoparticles for each concentration was added and stirred for 2 h in magnetic stirrer at 750–800 rpm. Later, the stirred sample was ultrasonicated for 2 h using Hielscher UP200H (200 W), at a frequency of 24 kHz to breakdown of agglomeration and to ensure the uniform and stable mixture of required concentration. As the nanofluid was found to be stable (observed visually and by thermal conductivity measurement), this method was followed for the preparation of nanofluids required for the study. Thereafter, nanofluids of different concentrations of CuO, Al_2O_3 and TiO_2 in EG:W mixture were prepared separately.

Measurement of thermal conductivity of nanofluid

Thermal conductivity of EG:W–CuO, Al_2O_3 and TiO_2 nanofluids was determined using KD2 Pro thermal properties analyser (Decagon Devices, Inc., USA). The instrument meets the requirements of ASTM D5334 and IEEE 442-1981 standards and has been used by various researchers [1–4, 29, 35, 36, 52, 53]. This instrument consists of a microcontroller and a KS-1 sensor needle with a size of 1.3 mm diameter and

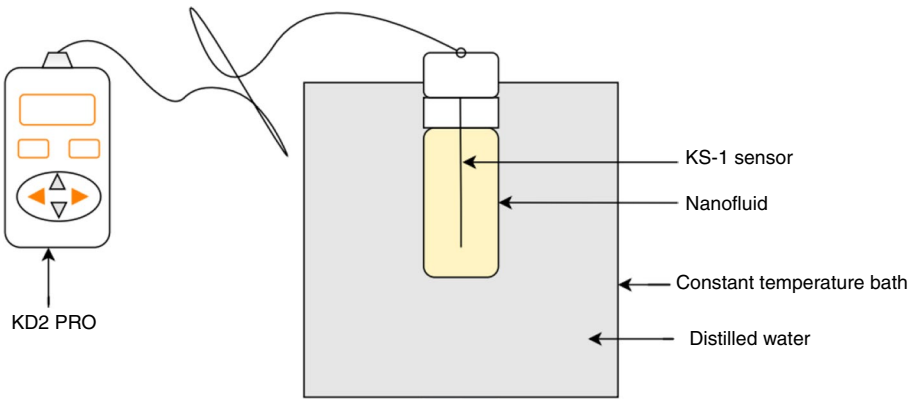

Fig. 1 Experimental arrangement for thermal conductivity measurement of nanofluids

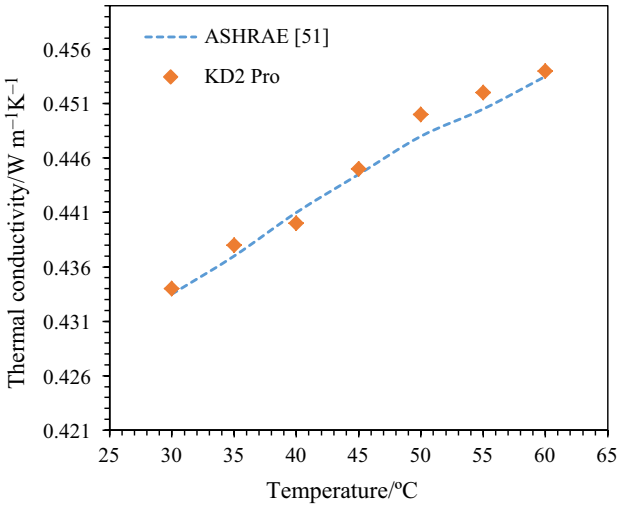

Fig. 2 Comparison of experimental results for k with ASHRAE data for EG:W mixture

6 cm long, capable of measuring the thermal conductivity in the range of 0.02–2.00 W m^{-1} K^{-1}. Prepared samples of specific nanofluid (volume = 30 mL) were taken in a glass tube of 30 mm diameter, which was equipped with a small opening (slightly larger than the sensor) through which the sensor needle was placed in it. The sensor was inserted into the fluid, oriented centrally and vertically inside the container without touching the side walls of the container as displayed in Fig. 1. Each nanofluid sample of CuO, Al_2O_3 and TiO_2 of different concentrations (0.2–2%) was taken into 30-mL glass bottle after preparation. Thermal conductivity at 30, 35, 40, 45, 50, 55 and 60 °C was measured in a constant temperature bath (TEMPO SM-1014). For each sample, five readings were taken by allowing 15 min for each reading for the temperature to equilibrate. The average of these readings was used for reporting the thermal conductivity of nanofluids. Figure 2 shows the comparison of thermal conductivity measurement with the ASHRAE data. The measured values show a maximum deviation of ± 2.5%.

Correlation for effective thermal conductivity

Considering experimental data from the present study

Thermal conductivity of nanofluids is dependent on the material of nanoparticle, base fluid, nanoparticle concentration, temperature and particle size. In the present study, the following correlation is proposed for predicting the effective thermal conductivity (ratio of k_{nf}/k_{bf}) of nanofluids (three nanopowders separately; diameter for each material is constant) as a function of nanofluid concentration and temperature based on the experimental data.

$$k_{\text{eff}} = \frac{k_{\text{nf}}}{k_{\text{bf}}} = A\left(\emptyset_{\text{m}}\right)^{\text{B}} \left(\frac{T_{\text{nf}}}{T_{\text{r}}}\right)^{\text{C}} \tag{2}$$

where k_{nf} and k_{bf} represent thermal conductivity of nanofluids and EG:water, respectively. T_{nf} and T_r represent the temperature of nanofluids and reference temperature (273.15 K). ϕ_m is mass fraction of nanofluids. A, B and C are the constants to be obtained after regression using experimental data.

Considering literature data

To develop more generalized correlations considering the experimental results from the present study and the results from literature reports, the following correlations (Eqs. (3) and (4)) are proposed. The effective thermal conductivity (k_{eff}) model of EG:W-based CuO, Al_2O_3 and TiO_2 proposed in Eq. (2) considers only temperature and mass concentration. The other parameters, viz., the volume ratio of EG:W mixture, temperature and size of nanoparticles which affect the thermal conductivity were not considered as they are kept constant. Two correlations, one material specific [Eq. (3)] and the other one [Eq. (4)] more general, considering the three materials, all the effecting variables and literature data, are proposed for k_{eff}.

$$k_{\text{eff}} = a\left(\emptyset_{\text{m}}\right)^{\text{b}} \left(V_{\text{r}}\right)^{\text{c}} \left(\frac{T_{\text{nf}}}{T_{\text{ref}}}\right)^{\text{d}} \left(\frac{d_{\text{np}}}{d_{\text{w}}}\right)^{\text{e}} \tag{3}$$

$$k_{\text{eff}} = a_1\left(\emptyset_{\text{m}}\right)^{b_1} \left(V_{\text{r}}\right)^{\text{c}_1} \left(\frac{T_{\text{nf}}}{T_{\text{ref}}}\right)^{\text{d}_1} \left(\frac{\text{d}_{np}}{\text{d}_{\text{w}}}\right)^{\text{e}_1} \left(\frac{k_{\text{np}}}{k_{\text{bf}}}\right)^{\text{f}_1} \tag{4}$$

where k_{eff} is effective thermal conductivity, $\emptyset_m$ = mass fraction of EG:W-based nanofluids, V_r = EG/water ratio (volume/volume), T_{nf} = the temperature of nanofluid in K, T_{ref} = reference temperature in K (273 K), d_{np} = nanoparticle diameter (nm), d_w = water molecule size in nm, k_{np} = thermal conductivity of nanoparticles (W m^{-1} K^{-1}), k_{bf} = thermal conductivity of the base fluid (W m^{-1} K^{-1}).

Artificial neural network (ANN) modelling

ANN modelling is a computational model based on the structure and functions of biological neural networks. Due

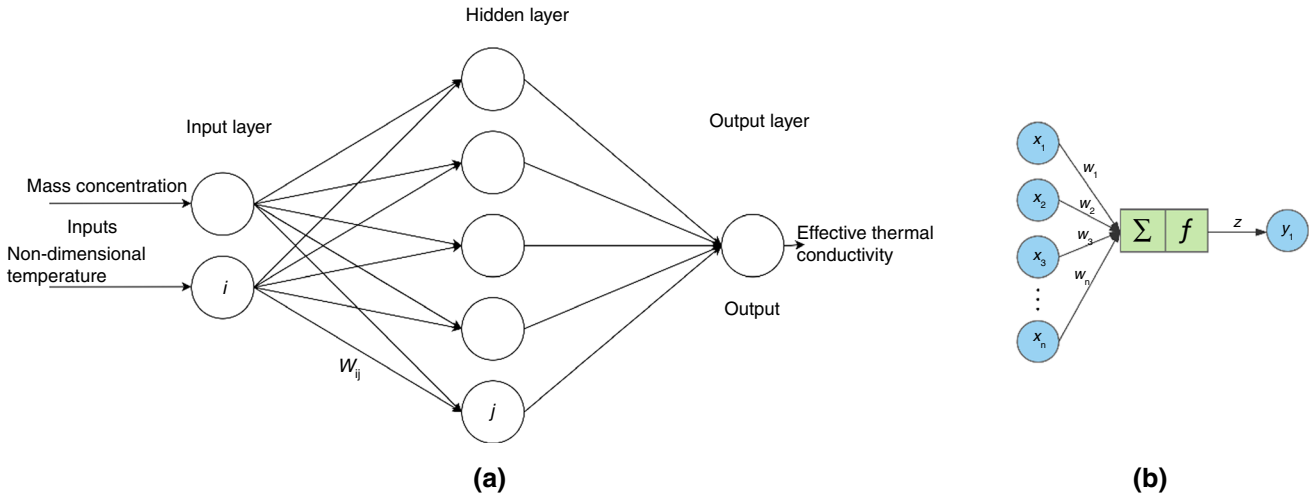

Fig. 3 ANN topology for the modelling of effective thermal conductivity

to the variation of data in a nonlinear pattern, achieving the output data prediction by the conventional method is quite difficult. ANN can provide better output by learning the nonlinear pattern of data through a modelled network. ANN modelling consists of three different layers with a number of neurons in each layer. Input neurons are the first layer (input layer), these neurons send data to the second layer (hidden layer), then output neuron to the third layer (output layer). The neurons in all layers are interconnected with each other with a mass coefficient as shown in Fig. 3a, b. Similar topology was used for the multiple variable input as used in Eqs. (3) and (4). Each neuron multiples these mass coefficients with a received input and adds up to get the output using a transfer function as shown in Fig. 3b. The processing of data takes place until the difference between the successive outputs data reaches a minimum. This can be represented in terms of ANN characterization parameters like masses (m), biases (b) and a function (f). The processing of output followed by the equation,

$$Y_{\mathrm{i}} = f\left(\sum_{i=1}^{n} w_{\mathrm{ij}} x_{\mathrm{i}} + b_{\mathrm{i}}\right) \tag{5}$$

where Y_{i}, x_{i} and n are the output, input and number of neurons that connect to the ith neuron, respectively. w_{ij} and b_{i} are the mass coefficients and bias, respectively. In this study, MLP-FF backpropagation ANN neural network containing three-layer perceptron was used. In order to optimize the results, hidden layers and neurons were varied to achieve a better prediction. This modelling process contains three objectives. (1) To compare the experimental data with the proposed Eq. (2) and ANN modelling (2) to optimize the ANN model to predict the effective thermal conductivity (material specific) considering the literature data and present experimental data, and comparing with regression Eq. (3) and (3) finally, to check the prediction of effective thermal conductivity considering present data and literature data of all materials (Table 1) together with Eq. (4) and ANN modelling.

Modelling was performed using NNTOOL in MATLAB software. The formulation of ANN modelling follows three steps, training, testing and validation. Training is the process of predicting appropriate masses and biases in order to recognize the specific relationship between the target and input functions. Levenberg–Marquardt learning algorithm was selected for learning process. Neural transfer functions used for hidden layer and output layer are tan-sigmoid and pure line, respectively. In this study, 75% of data (input) were randomly taken for training and the remaining 25% of data used for testing. The performance of model and regression equation prediction was evaluated using mean absolute deviation (MAD), mean square error (MSE) and mean absolute percentage error (MAPE) as follows.

$$\mathrm{MAD} = \frac{1}{N}\sum_{i=1}^{N}\left|Y_{\mathrm{e}} - Y_{\mathrm{p}}\right| \tag{6}$$

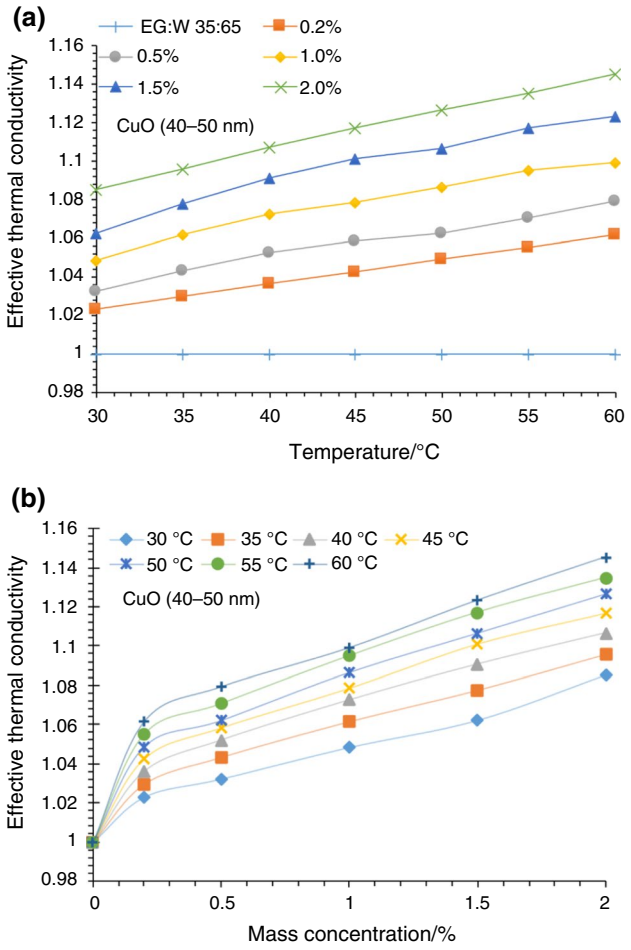

Fig. 4 **a** Effect of temperature on effective thermal conductivity for EG:W–CuO nanofluid, **b** effective thermal conductivity of EG:W–CuO nanofluids at a different mass concentrations

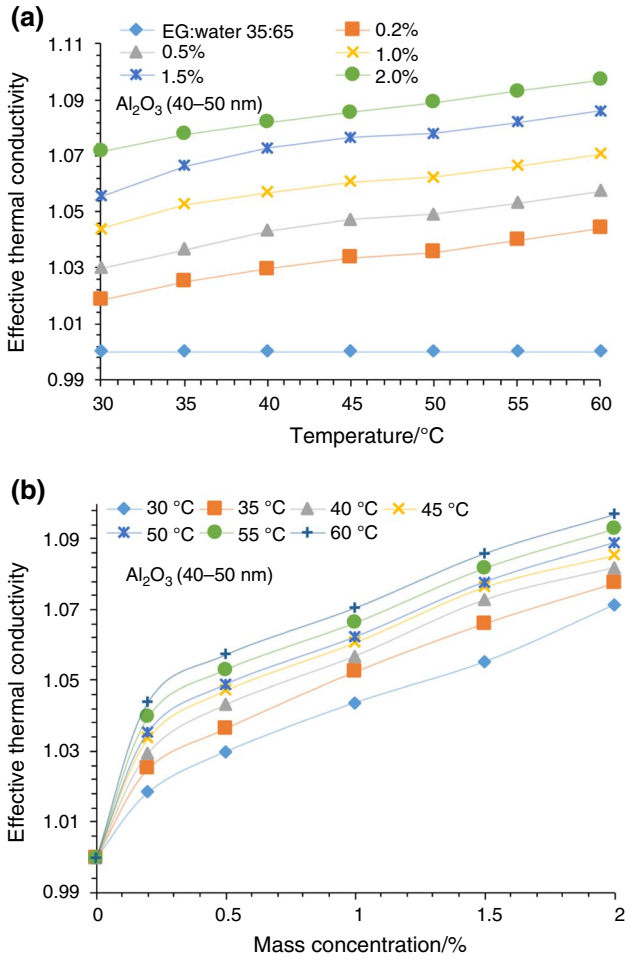

Fig. 5 **a** Effect of temperature on effective thermal conductivity for EG:W–Al_2O_3 nanofluid, **b** effective thermal conductivity of EG:W–Al_2O_3 nanofluid at a different mass concentrations

$$\mathrm{MSE} = \frac{1}{N}\sum_{i=1}^{N}\left(Y_\mathrm{e} - Y_\mathrm{p}\right)^2 \tag{7}$$

$$\mathrm{MAPE} = \frac{1}{N}\sum_{i=1}^{N}\left|\frac{Y_\mathrm{e} - Y_\mathrm{p}}{Y_\mathrm{e}} \times 100\right| \tag{8}$$

where Y_e, Y_p and N are the experimental value, predicted value from the ANN and number of data points.

Results and discussion

Effective thermal conductivity of nanofluids

In this study, thermal conductivity measurements at various temperatures (30, 35, 40, 45, 50, 55 and 60 °C) were carried out for nanoparticles of different materials (CuO, Al_2O_3 and TiO_2) with five different mass concentrations from 0 to 2%. Each measurement was repeated three times and the average value of the measurements was considered. The enhancement of thermal conductivity is presented in the form of effective thermal conductivity ($k_\mathrm{nf}/k_\mathrm{bf}$).

Figure 4a, b shows the effect of temperature and concentration on the effective thermal conductivity of EG:W–CuO nanofluids at different temperatures and mass concentrations. It can be observed from Fig. 4a that thermal conductivity increases to a maximum of 2.3% for 0.2% of concentration at 30 °C, and at 60 °C showed 6.16% enhancement compared to the base fluid. On the other hand, 2% mass concentration at 30 °C showed 8.53% of enhancement, and at 60 °C, it resulted in 14.53% enhancement.

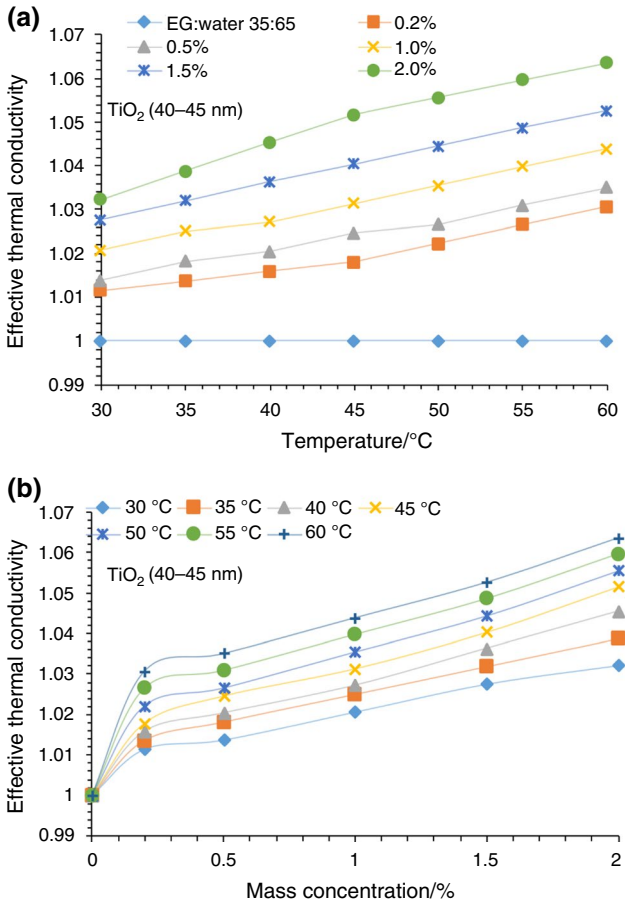

Fig. 6 **a** Effect of temperature on effective thermal conductivity for EG:W–TiO_2 nanofluid, **b** effective thermal conductivity of EG:W–TiO_2 nanofluids at a different mass concentrations

Figure 5a, b shows the effective thermal conductivity increase as a function of temperature for EG:W–Al_2O_3 nanofluids. From these figure, it can be observed that thermal conductivity enhancements were 1.84% and 4.40% for 0.2% concentration at 30 °C, and at 60 °C, respectively. On the other hand, nanofluid at 2% mass concentration showed an enhancement of 7.14% and 9.69% at 30 °C and 60 °C, respectively.

Figure 6a, b shows the effect of temperature and concentration on effective thermal conductivity with a temperature range of 30–60 °C for EG:W–TiO_2 nanofluids. The maximum thermal conductivity enhancement is 3.07% for 0.2 mass% mass concentration at 60 °C compared with base fluid (EG:W). Nanofluid of 2% mass concentration showed an enhancement of 3.22% and 6.35% at 30 °C and 60 °C, respectively.

The results showed a significant improvement in effective thermal conductivity due to the addition of nanoparticles. Thermal conductivity of EG:W-based nanofluid is higher than that of the base fluid at all concentrations. Thermal conductivity of nanofluids increases with temperature as in the case of the base fluid. Temperature and concentration of all nanofluids (CuO, Al_2O_3 and TiO_2) showed a significant effect on effective conductivity. Nevertheless, maximum enhancement was found at a higher concentration due to the higher thermal conductivity of solid particles. It can be observed from Figs. 4–6 that effective thermal conductivity increases with the temperature and concentration for all the nanofluids. A similar trend was also well reported in the literature for the CuO, Al_2O_3 and TiO_2 nanofluids [28, 29, 34, 35, 54].

Studies in literature indicate that aggregation of nanoparticles in suspensions influences thermal conductivity. To minimize the formation of agglomeration, sodium dodecyl benzene sulphonate (SDBS) surfactant was added in the present study. The addition of a surfactant is intended to help particles dispersed in base fluids. As a result of the addition of a surfactant, the particle agglomeration is reduced by the formation of a nanoparticle chain in the base fluid [55]. The enhancement of thermal conductivity with increased nanoparticle loading was due to the collisions between the particles. Brownian motion of nanoparticles increases at high fluid temperatures and the viscosity of nanofluid also decreases. With an increased Brownian motion, the role of micro-convection in heat transport increases which results in enhancement of thermal conductivity of nanofluids [29, 30, 35]. Another possible reason could be the nanolayer formation between the solid–liquid interfaces. The liquid molecules are known to form layered structures very near to

Table 5 Thermal conductivity enhancement (percentage) of EG:W-nanofluids for a temperature range of 30–60 °C

Nanoparticles	Nanoparticle concentration (mass%)				
	0.2	0.5	1	1.5	2
CuO (30–40 nm)	2.30–6.16	3.22–7.92	4.83–9.91	6.22–12.33	8.53–14.53
Al_2O_3(40–50 nm)	1.84–4.41	3–5.73	4.38–7.05	5.53–8.59	7.14–9.69
TiO_2(40–45 nm)	1.15–3.07	1.38–3.5	2.07–4.38	2.76–5.26	3.22–6.35

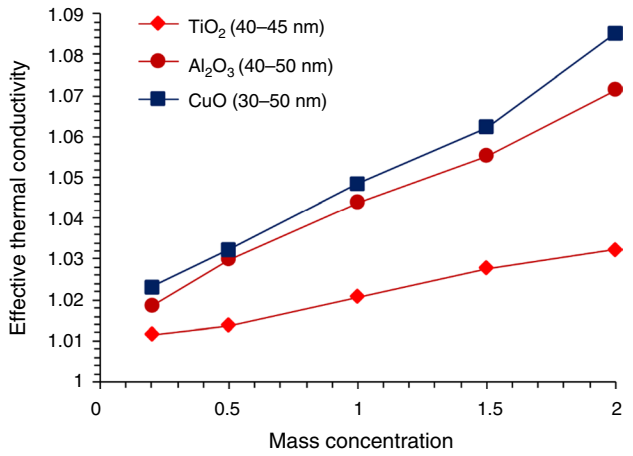

Fig. 7 Effect of three oxide nanopowders on effective thermal conductivity with respect to mass concentration at 30 °C

Table 6 A, B, C and R^2 values for Eq. (2)

Nanofluids	A	B	C	R^2
CuO/EG:water (35/65)	1.006	0.0286	0.495	0.944
Al_2O_3/EG:water (35/65)	1.024	0.0214	0.253	0.956
TiO_2/EG:water (35/65)	0.998	0.0118	0.243	0.915

Table 7 Performance of Eq. (2) in terms of deviation from experimental results

Nanofluids	Concentration (mass%)	% deviation (maximum and minimum) for k_e
CuO/EG:water(35/65)	0.2–2%	1.15 to −1.036
Al_2O_3/EG:water(35/65)	0.2–2%	0.57 to −0.73
TiO_2/EG:water(35/65)	0.2–2%	0.67 to −0.48

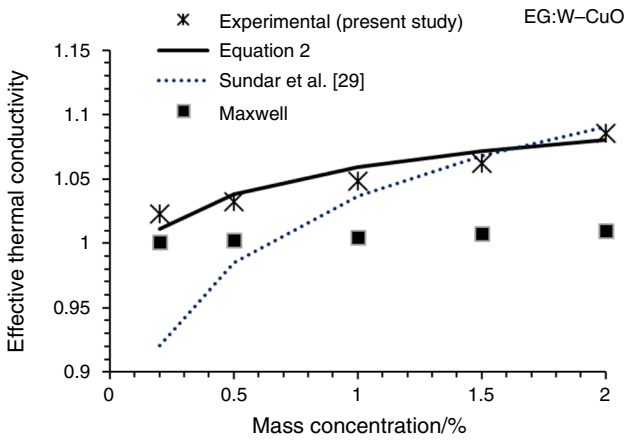

Fig. 8 Comparison of effective thermal conductivity of CuO nanofluid from the present study and literature models at 30 °C

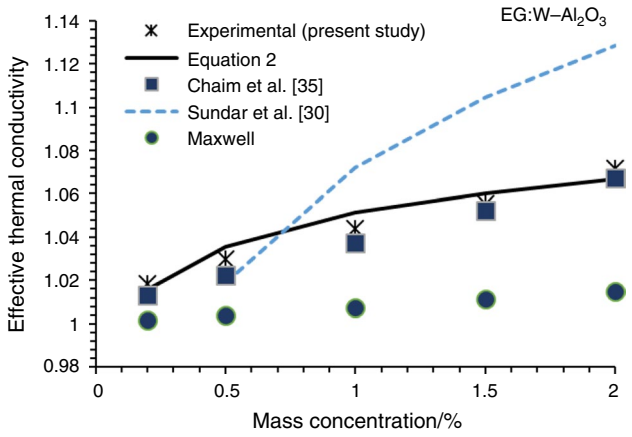

Fig. 9 Comparison of effective thermal conductivity of Al_2O_3 nanofluid from the present study and literature models at 30 °C

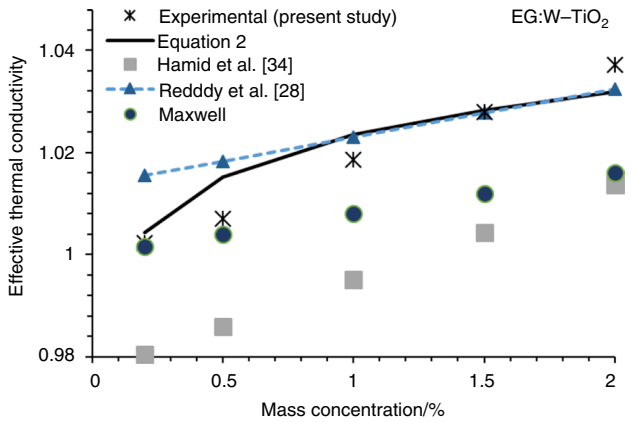

Fig. 10 Comparison of effective thermal conductivity of TiO_2 nanofluid from the present study and literature models at 30 °C

the particle surface and behave more like solid. The formation of these layer structures further creates a thermal bridge between the solid particles and liquid [36].

The effective thermal conductivity was maximum for the CuO nanofluids compared to Al_2O_3 and TiO_2 nanofluids as can be seen in Table 5 and Fig. 7. Al_2O_3 nanofluid showed better enhancement than the TiO_2 nanofluid. This can be attributed to the solid particles of the respective materials possessing higher thermal conductivity. However, it can also be observed that EG:W–Al_2O_3 nanofluid gives an enhancement of less than 4% as compared to the EG:W CuO nanofluids at 2 mass% of concentration. Due to its lower density, EG:W–Al_2O_3 can provide better stability compared to

EG:W–CuO nanofluids. The selection between these two materials has to be done considering all the above factors.

Development of correlation

Considering present experimental data

Regression was performed using experimental data to determine the correlation constants of A, B and C in Eq. (2). Correlation constants and R^2 values are given in Table 6. Performance of the model [Eq. (2)] was evaluated using the experimental data from the present study. The maximum and minimum deviations for the CuO, Al_2O_3 and TiO_2 nanofluids are reported in Table 7.

Validation of developed correlation

For predicting the results of the present study, the performance of the proposed correlation [Eq. (2)] was compared with the literature correlations for CuO, Al_2O_3 and TiO_2 nanoparticles in EG:W base fluid and with few classical mixture models. The comparison is shown in Figs. 8–10. It can be observed from Fig. 8 that at lower concentration Sundar et al. [29] correlation could not predict the effective thermal conductivity of EG:W–CuO which is used in the present study. This is due to the fact that the correlation developed by them was for higher concentration and 50:50 EG:W mixture. Figure 9 shows the comparison of k_{eff}, for Al_2O_3 nanoparticles. It can be seen that the model of Chiam et al. [35] performs better than the other two models. This may be attributed to the closer ratios of EG:W mixture (35:65 in the present study and 40:60 in Chiam et al.). Figure 10 shows the effective thermal conductivity comparison for EG:W–TiO_2 nanofluids. The studies by Hamid et al. [34] and Reddy et al. [28] involved different particle size, base fluid ratio and concentration. The experimental results from the present study showed higher thermal conductivity than the models proposed by Maxwell for all mass concentrations

Table 8 Regression constants and R^2 value for Eq. 3

Nanofluids	A	B	C	D	E	R^2
CuO/EG:water	0.9972	0.0345	− 0.0161	0.4980	0.0009	0.846
Al_2O_3/EG:water	0.7464	0.06754	− 0.0156	0.6235	0.0563	0.831
TiO_2/EG:water	0.8687	0.1823	0.0703	0.1754	0.3633	0.663

Table 9 Regression constants and R^2 value for Eq. 4

Nanofluids	A_1	B_1	C_1	D_1	E_1	F_1	R^2
Considering all materials	0.7085	0.0584	0.0011	0.5182	0.0537	0.0177	0.6923

Table 10 ANN modelling results for EG:W-based nanofluids considering present experimental results

Number of hidden layers	Neurons in hidden layer	Modelling coefficient, R				Mean square error (MSE)
		Training data	Validating data	Testing data	All data	
EG:W–CuO nanofluid						
1	6	0.9991	0.9989	0.9996	0.9906	9.89E−06
1	**8**	**0.9994**	**0.9997**	**0.9999**	**0.9995**	**9.90937E−07**
1	10	0.9944	0.9990	0.9993	0.9952	1.89434E−06
EG:W–Al_2O_3 nanofluid						
1	6	0.9995	0.9996	0.9875	0.9983	2.26545E−06
1	**8**	**0.9995**	**0.9996**	**0.9999**	**0.9994**	**5.16249E−07**
1	10	0.9962	0.9961	0.9984	0.9976	1.44601E−06
EG:W–TiO_2 nanofluid						
1	6	0.9989	0.9973	0.9994	0.9986	7.01276E−07
1	**8**	**0.9994**	**0.9992**	**0.9995**	**0.9993**	**2.6111E−07**
1	10	0.9974	0.9996	0.9998	0.9980	5.51832E−07

Bold indicates Optimized result obtained for the ANN Modeling

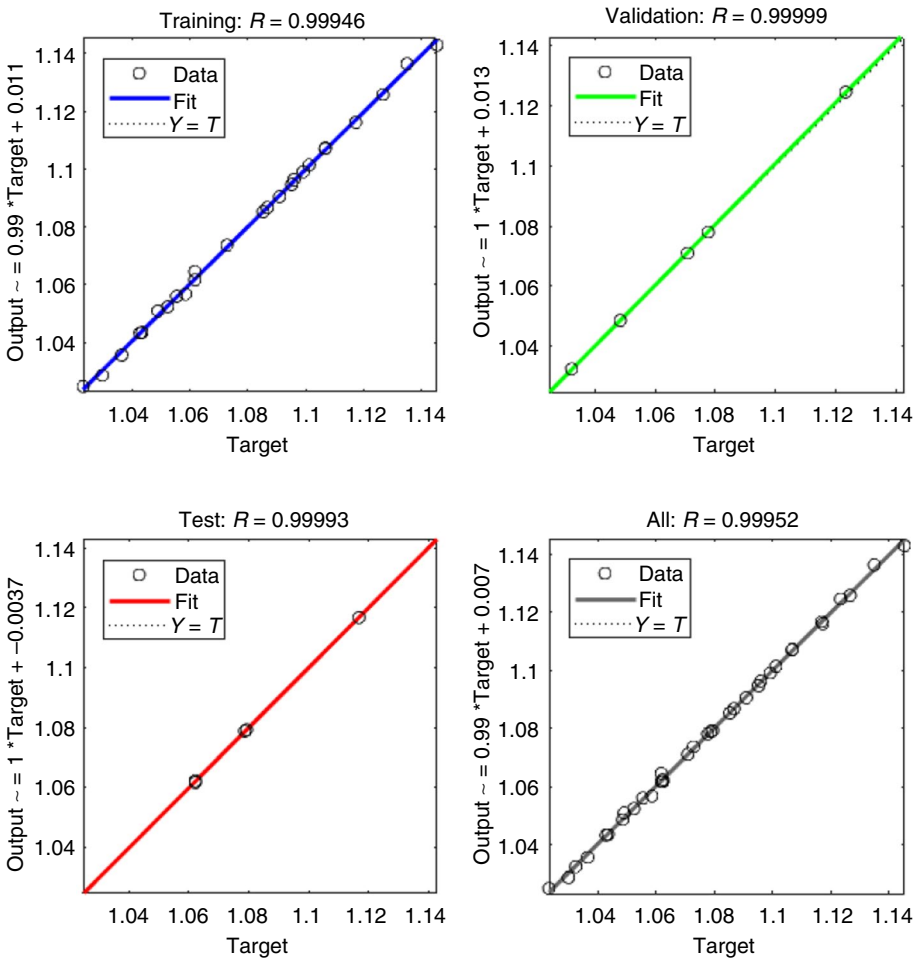

Fig. 11 Optimized ANN modelling regression for EG:W–CuO nanofluid

(Figs. 8–10). It has been observed that thermal conductivity increases with an increase in mass concentration in both experimental data and developed models. However, the calculated thermal conductivity for all nanofluids by the Maxwell model is lower than the current experimental data. This is due to the fact that the classical model does not consider other factors affecting thermal conductivity, such as the interaction between the particle and the liquid, size of the particle, the Brownian motion of the particles and the aggregation of the particles.

Considering literature data

The correlation proposed previously [Eq. (2)] considers temperature and concentration only. However, thermal conductivity also depends on the factors such as volume ratio of EG:W, nanoparticle size and thermal conductivity of nanoparticles. Therefore, considering all the factors regression was carried out for Eq. (3) using the experimental results from the present study and literature, for the three materials separately. Regression constants and correlation coefficients are given in Table 8. Subsequently, a generalized equation was developed for all the materials (Eq. (4); Table 9). It can be seen from Tables 8 and 9 that, the fit is better for individual materials than the combined correlation (as indicated by R^2 values).

ANN modelling

Considering present experimental data

The regression for Eq. (2) gave a regression coefficient of about 0.95. For a better prediction, MLP-ANN modelling was carried out to predict the effective thermal conductivity. Experimental results were used as a target for training and validating with the input data. Neural networks with a single hidden layer with 6, 8 and 10 neurons were tried for modelling the experimental results. Table 10 shows the

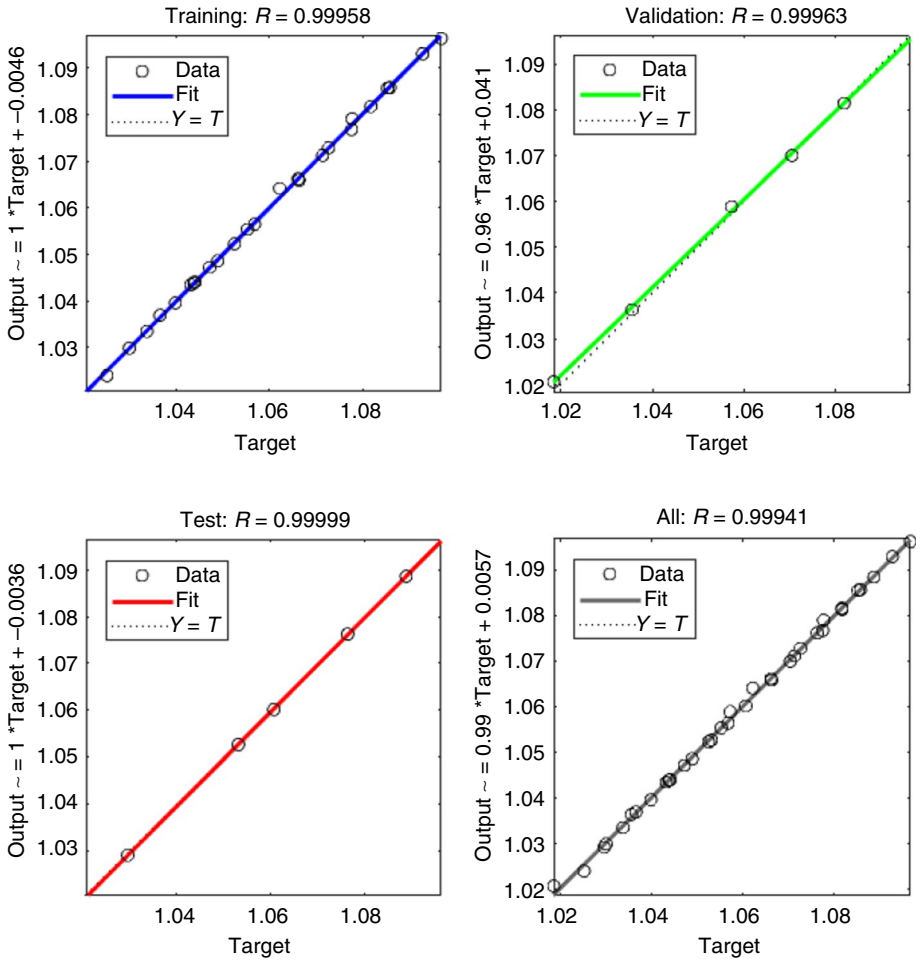

Fig. 12 Optimized ANN modelling regression for EG:W–Al_2O_3 nanofluid

ANN modelling results for the aforementioned neural network. The modelling coefficient (R) between the yield model and the training set, validation set, testing set and finally the entire experimental data are shown in Table 10 for evaluation criteria. It can be observed from the tables that, ANN modelling with less number of neurons in a single hidden layer predicts effective thermal conductivity for all materials with limited data. However, eight neurons in a single hidden layer structure were considered to present the ANN modelling result due to the optimum value of the MSE and modelling coefficient as shown in Table 10.

The prediction of effective thermal conductivity of CuO, Al_2O_3 and TiO_2 nanofluids from ANN modelling is shown in Figs. 11–13, respectively, for eight hidden neurons in a single hidden layer of neural network. The predicted data of effective thermal conductivity obtained from ANN are compared with the experimental data and Eq. (2) as shown in Figs. 14–16. From these figures, it can be seen that prediction of the results by ANN is significantly better. ANN modelling and Eq. (2) are further compared in terms of different parameters of error such as MAD, MSE and MAPE in Table 11. It can be seen from Table 11 that ANN modelling provides a minimum MAD, MSE and MAPE compared to Eq. (2) for all the nanofluid.

Considering present experimental data and literature data

Modelling was carried out previously using experimental results from the present study only, considering non-dimensional temperature and concentration as input variables. Equation (3) was proposed for performing the regression considering the literature data with each material separately. The values of the regression coefficient for Eq. (3) obtained for all three materials are significantly less than 1 (shown in

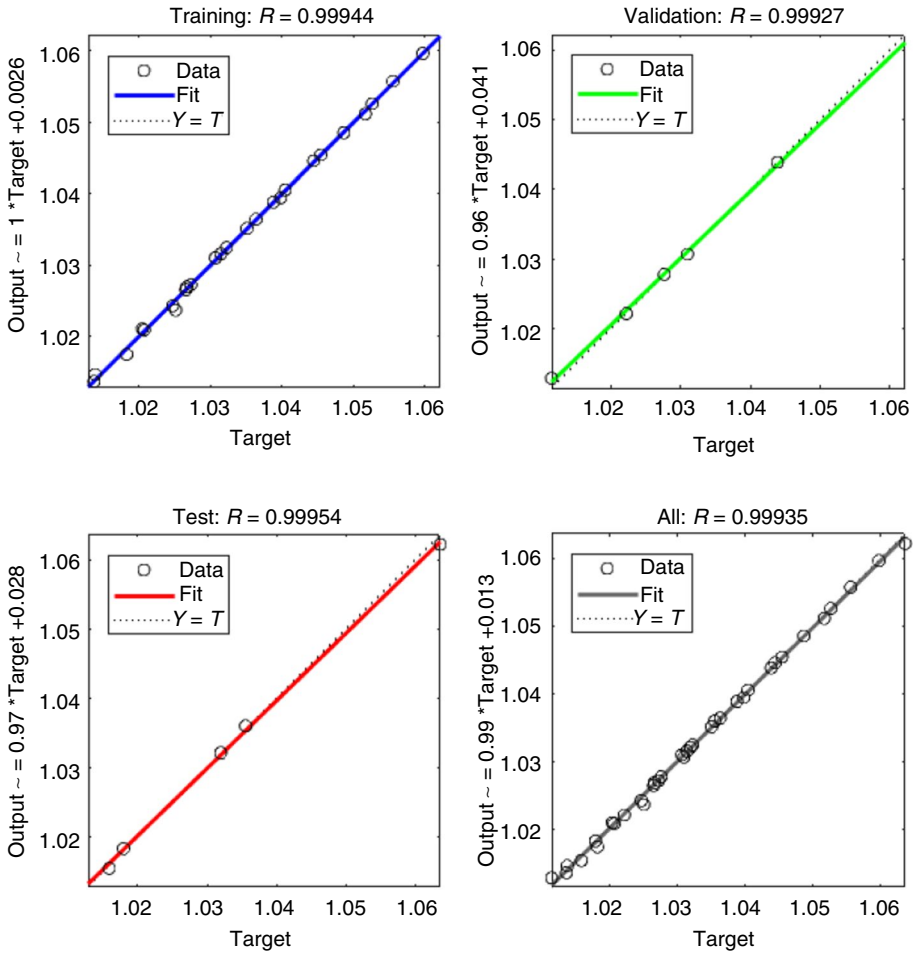

Fig. 13 Optimized ANN modelling regression for EG:W–TiO_2 nanofluid

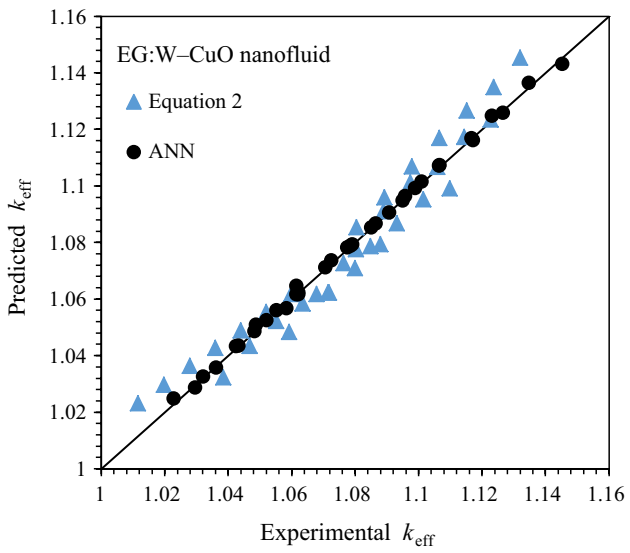

Fig. 14 Effective thermal conductivity of ANN and proposed correlation comparison for EG:W–CuO nanofluid

Table 8) indicating scope for a better model. Artificial neural network (ANN) modelling was carried out considering the results from the present study and literature data.

Table 12 shows the results for different configurations used to determine the optimum neural network for predicting the thermal conductivity of EG:W nanofluids for each material separately. Table 12 shows the results for different hidden layer neurons for EG:W nanofluids of three materials. The single hidden layer with neurons 10, 12 and 6 (CuO, Al_2O_3 and TiO_2) gave optimized results with minimum MSE. The corresponding optimized ANN results are shown in Figs. 17–19. These results were compared with the experimental, literature results and Eq. (3) as shown in Figs. 20–22. It can be observed from the figure that ANN modelling performs better prediction than Eq. (3) for EG:W nanofluids with large amount of data.

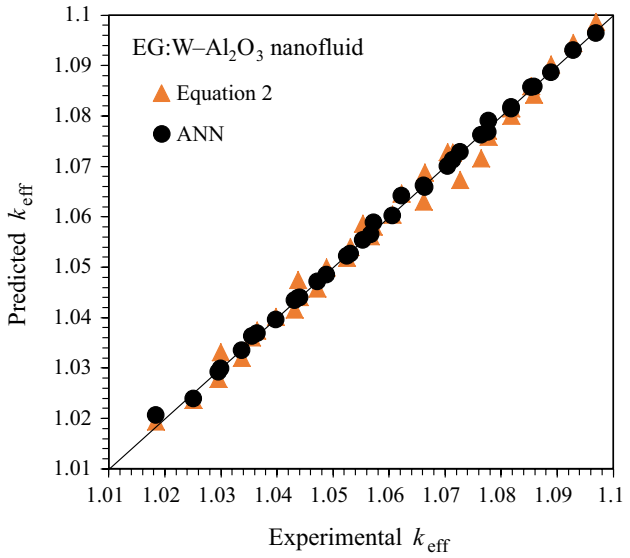

Fig. 15 Effective thermal conductivity of ANN and proposed correlation comparison for EG:W–Al_2O_3 nanofluid

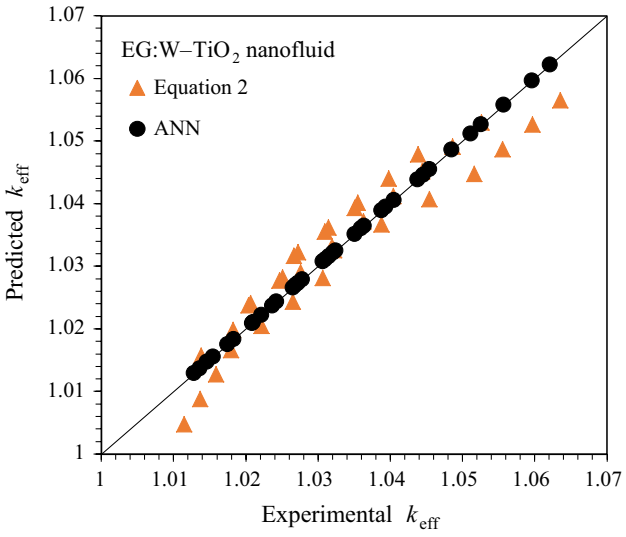

Fig. 16 Effective thermal conductivity of ANN and proposed correlation comparison for EG:W–TiO_2 nanofluid

Table 11 Statistics for ANN model and Eq. (2) considering present experimental results

Nanofluids	Parameter	ANN1	ANN2	ANN3	Equation 2
EG:water–CuO nanofluid	MAD	0.001958455	**0.000678798**	0.0009955	0.006586729
	MSE	9.89E−06	**9.90937E−07**	1.89434E−06	5.5346E−05
	MAPE	0.181656095	**0.062891454**	0.091452255	0.61105645
EG:water–Al_2O_3 nanofluid	MAD	0.001073382	**0.000490243**	0.000815411	0.001656144
	MSE	2.26545E−06	**5.16249E−07**	1.44601E−06	4.29069E−06
	MAPE	0.102016608	**0.04651602**	0.077191945	0.156165154
EG:water–TiO_2 nanofluid	MAD	0.000574702	**0.000331364**	0.000555925	0.003303173
	MSE	7.01276E−07	**2.6111E−07**	5.51832E−07	1.53109E−05
	MAPE	0.055545076	**0.032167215**	0.053765712	0.319161647

Bold indicates Optimized result obtained for the ANN Modeling

Table 12 ANN modelling results for EG:W-based nanofluids considering literature data

Number of hidden layers	Neurons in hidden layer	Modelling coefficient/*R*				Mean square error (MSE)
		Training data	Validating data	Testing data	All data	
EG:W–CuO nanofluid						
1	6	0.9987	0.9984	0.9972	0.9982	4.83493E−06
1	8	0.9984	0.9998	0.9956	0.9982	5.45949E−06
1	**10**	**0.9999**	**0.9994**	**0.9988**	**0.9996**	**9.65737E−07**
1	12	0.9987	0.9983	0.9988	0.9986	3.5931E−06
1	14	0.9938	0.9990	0.9995	0.9952	1.47656E−05
EG:W–Al_2O_3 nanofluid						
1	6	0.9958	0.9896	0.9962	0.9955	5.13964E−05
1	8	0.9973	0.9962	0.9981	0.9973	3.10183E−05
1	10	0.9973	0.9990	0.9980	0.9977	2.65014E−05
1	**12**	**0.9990**	**0.9984**	**0.9990**	**0.9988**	**1.28201E−05**
1	14	0.9977	0.9966	0.9971	0.9974	2.97659E−05
1	16	0.9972	0.9978	0.9982	0.9974	2.89707E−05
EG:W–TiO_2 nanofluid						
1	4	0.9978	0.9981	0.9983	0.9980	6.93419E−06
1	5	0.9990	0.9995	0.9979	0.9990	3.45053E−06
1	**6**	**0.9994**	**0.9990**	**0.9983**	**0.9993**	**2.4378E−06**
1	8	0.9986	0.9998	0.9997	0.9988	4.2636E−06
1	10	0.9990	0.9997	0.9987	0.9991	3.08792E−06

Bold indicates Optimized result obtained for the ANN Modeling

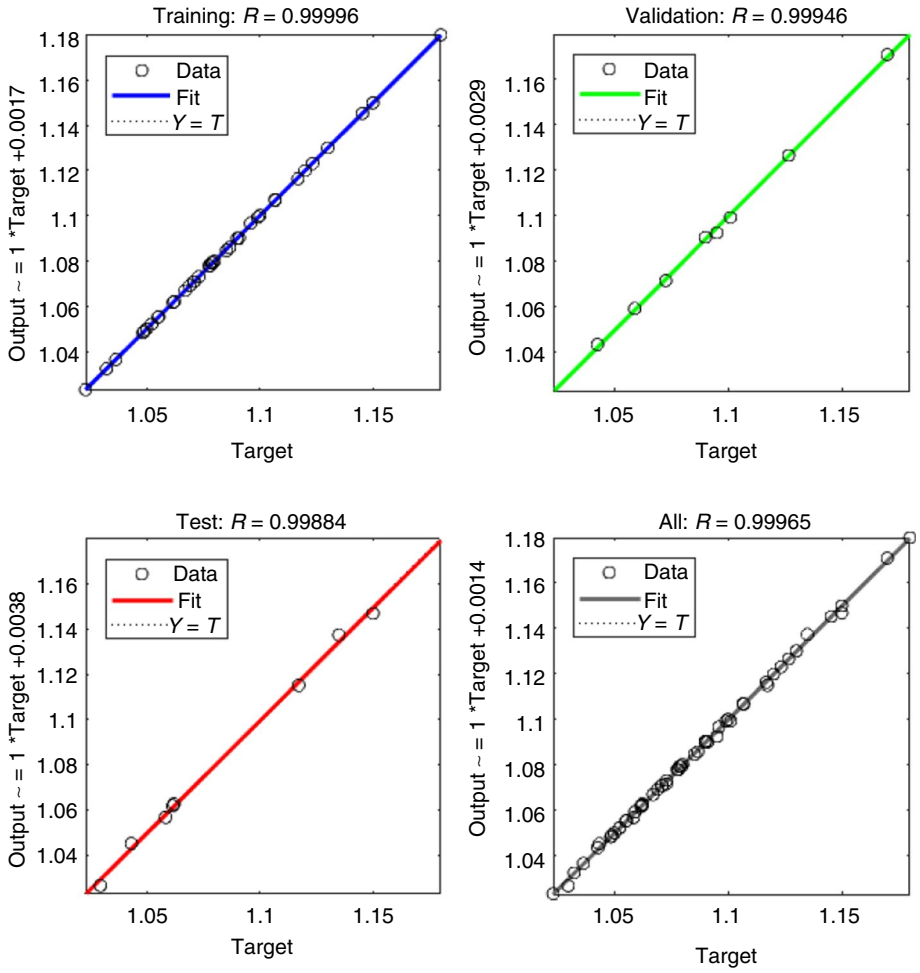

Fig. 17 Optimized ANN modelling of EG:W–CuO nanofluids considering literature data

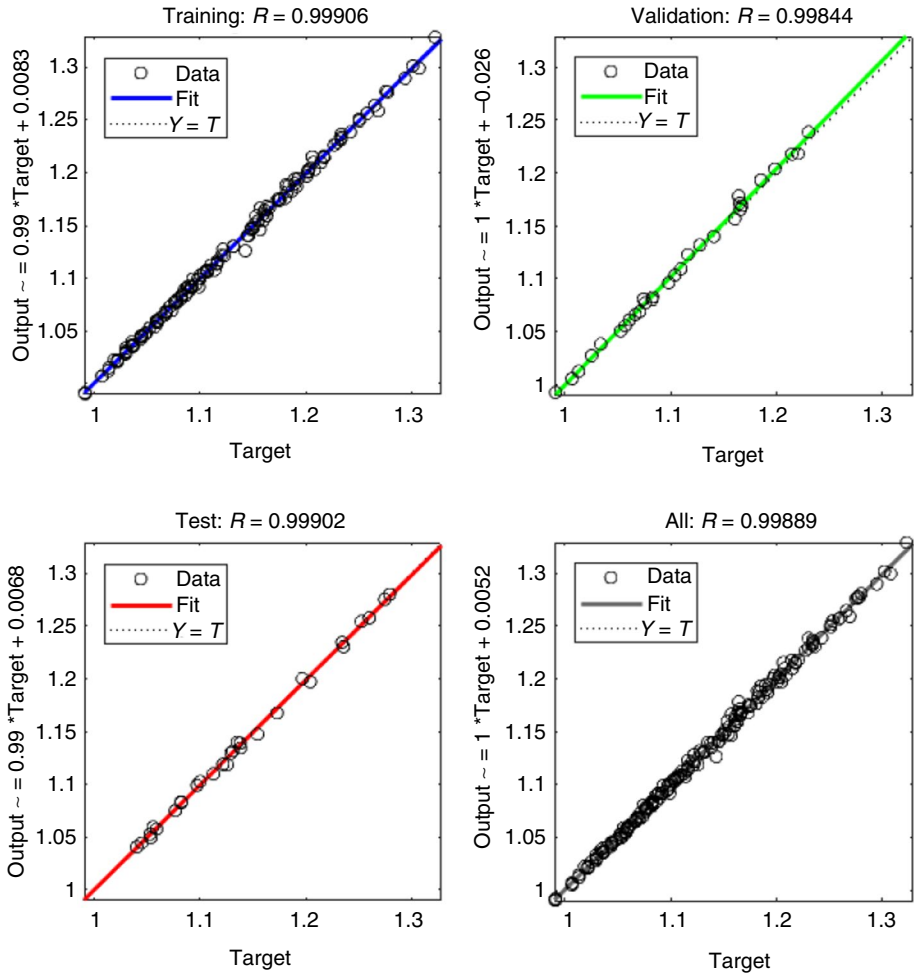

Fig. 18 Optimized ANN modelling of EG:W–Al_2O_3 nanofluids considering literature data

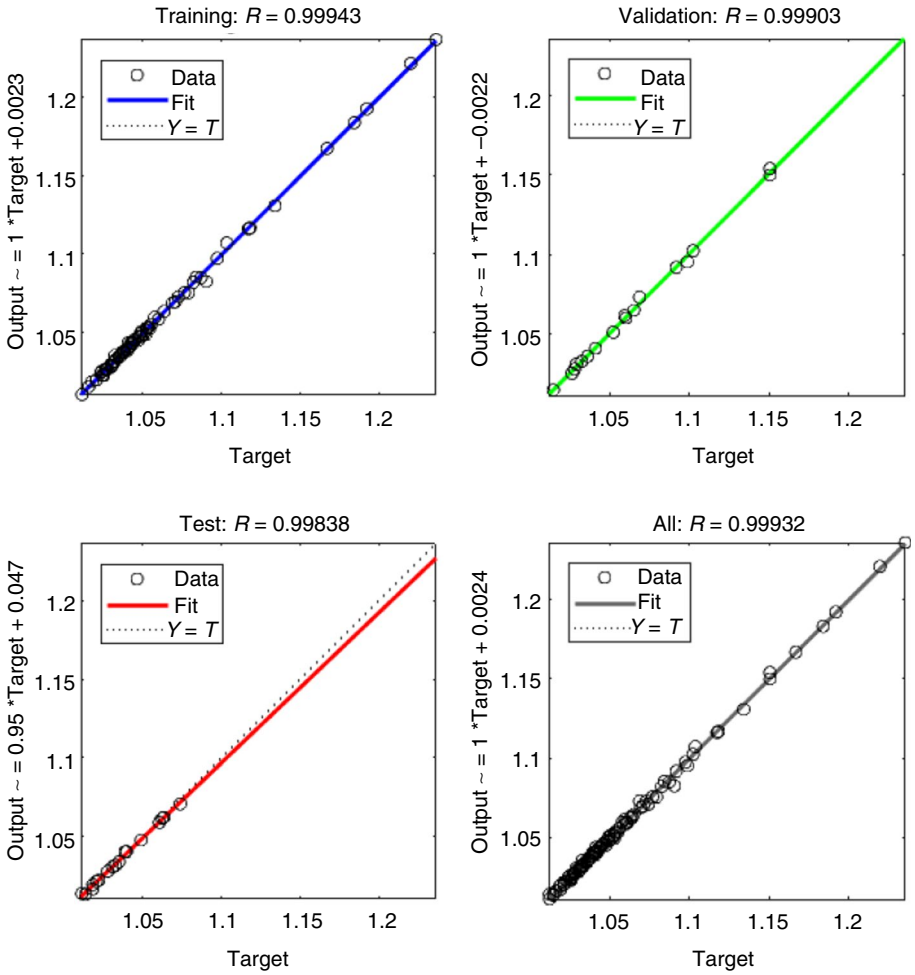

Fig. 19 Optimized ANN modelling of EG:W–TiO_2 nanofluids considering literature data

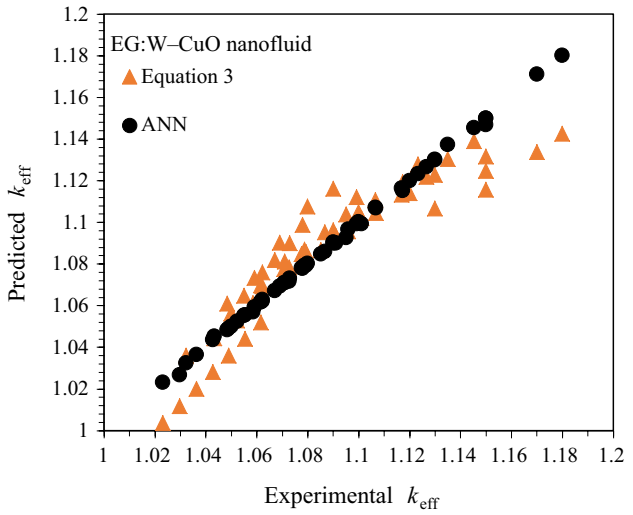

Fig. 20 Comparison of ANN model and Eq. (3) with present data and literature data of EG:W–CuO nanofluid

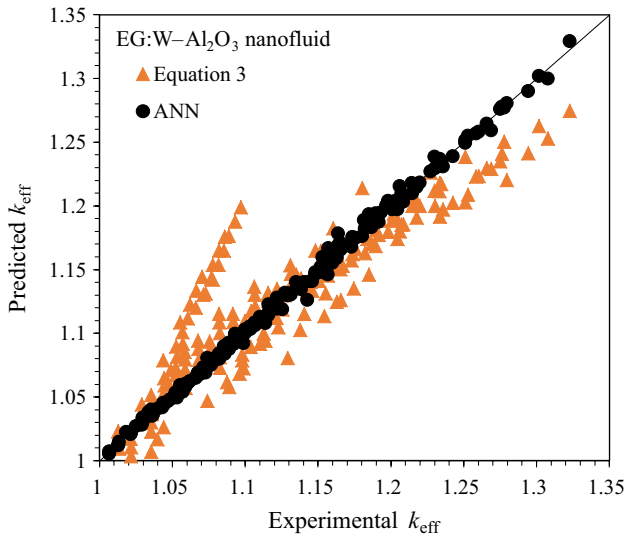

Fig. 21 Comparison of ANN model and Eq. (3) with present data and literature data of EG:W–Al_2O_3 nanofluid

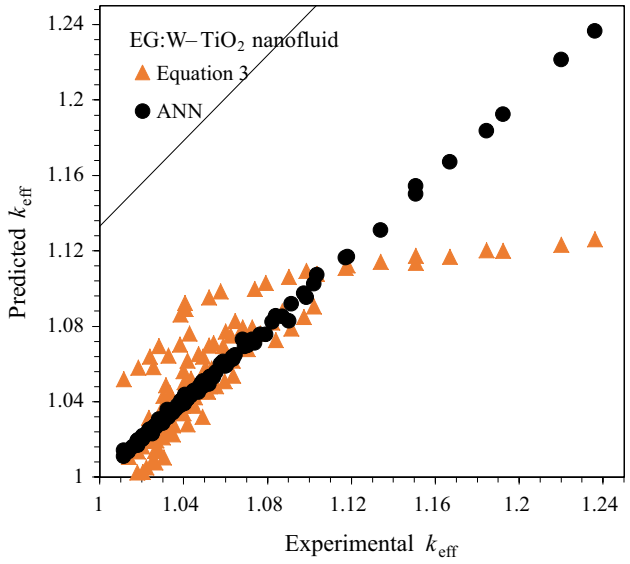

Fig. 22 Comparison of ANN model and Eq. (3) with present data and literature data of EG:W–TiO_2 nanofluid

Considering literature data and present data of all materials together

The generalized Eq. (4) developed previously from the regression is not satisfactory since the R^2 value is 0.693 (Table 9). Therefore, ANN modelling was carried out considering the same input parameters in a non-dimensional form as used in Eq. (4) and effective thermal conductivity as output. In this case, it is important to optimize the hidden layer neurons as the input variables are more compared to previous case. Hence, the optimization of neural network structure was carried out using both single and two hidden layers with varying the neurons. Table 13 gives the details of the hidden layer with different neurons. The neural network with two hidden layers containing twelve neurons was found to have the least MSE and therefore the most favourable structure for modelling the effective thermal conductivity. Figure 23 shows the performance of optimized number of neurons from ANN modelling. ANN results so obtained are compared with Eq. (4) in Fig. 24. ANN modelling shows better prediction than Eq. (4). The effect of five parameters

Table 13 ANN modelling results for EG:W-based nanofluids considering literature data and present study for the three nanofluids

Number of hidden layers	Neurons in hidden layer	Modelling coefficient *R*				Mean square error (MSE)
		Training data	Validating data	Testing data	All data	
1	6	0.9953	0.9975	0.9964	0.9959	3.84264E−05
1	8	0.9990	0.9972	0.9952	0.9967	3.13433E−05
1	10	0.9960	0.9968	0.9975	0.9964	3.40371E−05
1	12	0.9971	0.9973	0.9954	0.9969	2.91289E−05
1	14	0.9971	0.9973	0.9954	0.9969	3.04394E−05
1	17	0.9976	0.9970	0.9972	0.9974	2.4304E−05
1	20	0.9975	0.9982	0.9984	0.9977	2.19906E−05
1	23	0.9975	0.9964	0.9958	0.9969	2.94666E−05
2	8	0.9959	0.9976	0.9961	0.9962	3.55855E−05
2	10	0.9958	0.9961	0.9971	0.9961	3.7024E−05
2	**12**	**0.9983**	**0.9983**	**0.9978**	**0.9981**	**1.73518E−05**
2	14	0.9974	0.9969	0.9958	0.9970	2.8081E−05
2	16	0.9970	0.9988	0.9958	0.9970	2.82528E−05

Bold indicates Optimized result obtained for the ANN Modeling

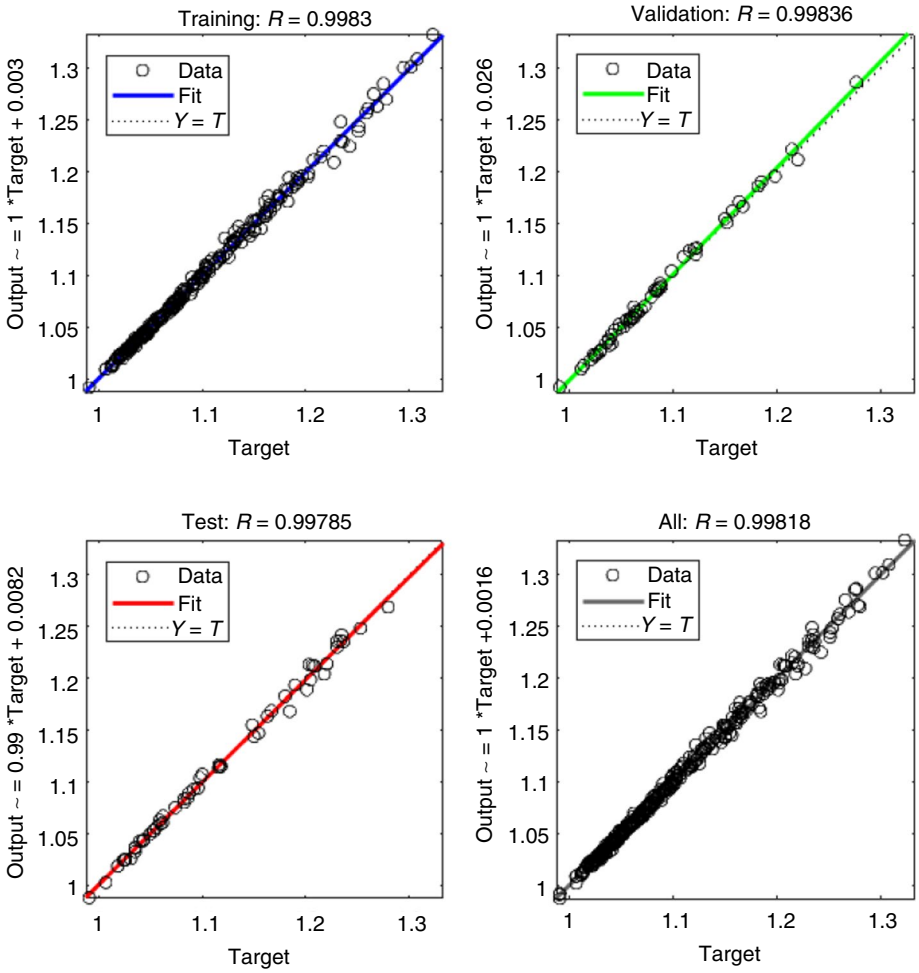

Fig. 23 Optimized ANN modelling of EG:W nanofluids considering literature data of three materials

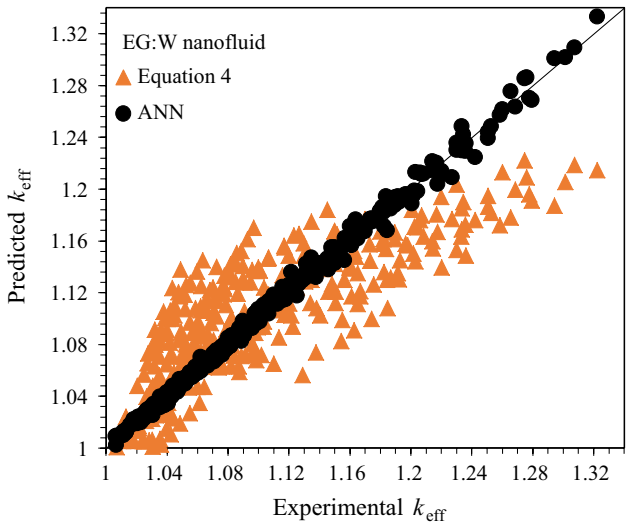

Fig. 24 Comparison of ANN and correlation developed considering literature data and present study

on effective thermal conductivity for a wide range of data (literature and current data) can be obtained from the optimized neural network. Thus, the neural network structure of the MLP offers an efficient way to predict the properties of nanofluids over a wide range of conditions.

Conclusions

In this study, the effective thermal conductivity of CuO, Al_2O_3 and TiO_2 nanoparticles dispersed in EG:W mixture of 35/65 volume by volume was investigated. Results showed that thermal conductivity of EG:W nanofluids is higher compared to the base fluid. Thermal conductivity of the nanofluid follows the same trend as that of the EG:W mixture and increases with temperature. The maximum enhancement of thermal conductivity for CuO, Al_2O_3 and TiO_2 nanoparticles in EG:W mixture was 8.53%, 7.14% and 3.22% at 30 °C and 14.54%, 9.69% and 6.35% at 60 °C, respectively, for 2% of mass concentration. Empirical correlations for CuO, Al_2O_3 and TiO_2 in 35:65 ratio of EG:W mixture were developed. The proposed correlation

predicted the experimental results with a deviation of ± 1.16%. However, ANN modelling improved the prediction compared to the correlation. Subsequently, literature data for EG:W mixture-based CuO, Al_2O_3 and TiO_2 nanofluids were considered to develop the correlation separately for the three materials. Further, a generalized correlation (for three materials) was developed considering literature data which gave R^2 values of 0.846, 0.831 and 0.663 for CuO, Al_2O_3 and TiO_2 nanofluids, respectively, and generalized correlation for all materials R^2 of 0.692. Prediction was significantly improved for all the above cases by ANN modelling. Hence, the effect of several influencing factors on effective thermal conductivity can be modelled using optimized neural network for a wide range of data. Therefore, the neural network structure of the MLP can be considered as a reliable tool for modelling experimental data of nanofluids.

Acknowledgements The financial support by Aeronautical Research and Development (AR&DB) under Grant No. of ARDB/01/2031857/M/I is gratefully acknowledged.

References

1. Srinivas T, Vinod AV. The effective thermal conductivity of water based nanofluids at different temperatures. J Test Eval. 2016;44:280–9.
2. Naik BAK, Vinod AV. Rheological behavior and effective thermal conductivity of non-Newtonian nanofluids. J Test Eval. 2018;46:445–57.
3. Yashawantha KM, Afzal A, Ramis MK, Shareefraza JU. Experimental investigation on physical and thermal properties of graphite nanofluids. In: AIP conference proceedings. 2018. p. 020057.
4. Yashawantha KM, Asif A, Ravindra Babu G, Ramis MK. Rheological behavior and thermal conductivity of graphite–ethylene glycol nanofluid. J Test Eval. 2021;49:Published ahead of print.
5. Ukkund SJ, Ashraf M, Udupa AB, Gangadharan M, Pattiyeri A, Marigowda YK, et al. Synthesis and characterization of silver nanoparticles from *Fusarium oxysporum* and investigation of their antibacterial activity. Mater Today Proc. 2019;9:506–14.
6. Masuda H, Ebata A, Teramae K. Alteration of thermal conductivity and viscosity of liquid by dispersing ultra-fine particles. Dispersion of Al_2O_3, SiO_2 and TiO_2 ultra-fine particles. Netsu Bussei. 1993;7:227–33.
7. Michael M, Zagabathuni A, Ghosh S, Pabi SK. Thermo-physical properties of pure ethylene glycol and water–ethylene glycol mixture-based boron nitride nanofluids: an experimental investigation. J Therm Anal Calorim. 2019;137:369–80.
8. Barbés B, Páramo R, Blanco E, Pastoriza-Gallego MJ, Piñeiro MM, Legido JL, et al. Thermal conductivity and specific heat capacity measurements of Al_2O_3 nanofluids. J Therm Anal Calorim. 2013;111:1615–25.
9. Hemmat Esfe M, Saedodin S, Wongwises S, Toghraie D. An experimental study on the effect of diameter on thermal conductivity and dynamic viscosity of Fe/water nanofluids. J Therm Anal Calorim. 2015;119:1817–24.
10. Hemmat Esfe M, Saedodin S, Asadi A, Karimipour A. Thermal conductivity and viscosity of $Mg(OH)_2$–ethylene glycol nanofluids. J Therm Anal Calorim. 2015;120:1145–9.
11. Meyer JP, Adio S, Sharifpur M, Nwosu PN. The viscosity of nanofluids: a review of the theoretical, empirical and numerical models. Heat Transf Eng. 2015;37(5):387–421.
12. Ramesh G, Prabhu NK. Review of thermo-physical properties, wetting and heat transfer characteristics of nanofluids and their applicability in industrial quench heat treatment. Nanoscale Res Lett. 2011;6:334.
13. Sajid MU, Ali HM. Recent advances in application of nanofluids in heat transfer devices: a critical review. Renew Sustain Energy Rev. 2019;103:556–92.
14. Huminic G, Huminic A. Application of nanofluids in heat exchangers: a review. Renew Sustain Energy Rev. 2012;16:5625–38.
15. Ghozatloo A, Rashidi A, Shariaty-Niassar M. Convective heat transfer enhancement of graphene nanofluids in shell and tube heat exchanger. Exp Thermal Fluid Sci. 2014;53:136–41.
16. Shahrul IM, Mahbubul IM, Saidur R, Sabri MFM. Experimental investigation on Al_2O_3–W, SiO_2–W and ZnO–W nanofluids and their application in a shell and tube heat exchanger. Int J Heat Mass Transf. 2016;97:547–58.
17. Kareemullah M, Chethan KM, Fouzan MK, Darshan BV, Kaladgi AR, Prashanth MB, et al. Heat transfer analysis of shell and tube heat exchanger cooled using nanofluids. Recent Patents Mech Eng. 2019;12:350–6.
18. Khairul MA, Saidur R, Rahman MM, Alim MA, Hossain A, Abdin Z. Heat transfer and thermodynamic analyses of a helically coiled heat exchanger using different types of nanofluids. Int J Heat Mass Transf. 2013;67:398–403.
19. Fule PJ, Bhanvase BA, Sonawane SH. Experimental investigation of heat transfer enhancement in helical coil heat exchangers using water based CuO nanofluid. Adv Powder Technol. 2017;28:2288–94.
20. Teng TP, Hsiao TC, Chung CC. Characteristics of carbon-based nanofluids and their application in a brazed plate heat exchanger under laminar flow. Appl Therm Eng. 2019;146:160–8.
21. Wang Z, Wu Z, Han F, Wadsö L, Sundén B. Experimental comparative evaluation of a graphene nanofluid coolant in miniature plate heat exchanger. Int J Therm Sci. 2018;130:148–56.
22. Eastman JA, Choi US, Li S, Thompson LJ, Lee S. Enhanced thermal conductivity through the development of nanofluids. In: Materials research society symposium—proceedings. 1997. p. 3–11.
23. Eastman JA, Choi SUS, Li S, Yu W, Thompson LJ. Anomalously increased effective thermal conductivities of ethylene glycol-based nanofluids containing copper nanoparticles. Appl Phys Lett. 2001;78:718–20.
24. Yu W, Xie H, Chen L, Li Y. Investigation of thermal conductivity and viscosity of ethylene glycol based ZnO nanofluid. Thermochim Acta. 2009;491:92–6.
25. Azmi WH, Hamid KA, Usri NA, Mamat R, Sharma KV. Heat transfer augmentation of ethylene glycol: water nano fluids and applications—a review. Int Commun Heat Mass Transfr. 2016;75:13–23.
26. Vajjha RS, Das DK. Experimental determination of thermal conductivity of three nanofluids and development of new correlations. Int J Heat Mass Transf. 2009;52:4675–82.
27. Kole M, Dey TK. Investigation of thermal conductivity, viscosity, and electrical conductivity of graphene based nanofluids. J Appl Phys. 2013;113:084307.
28. Reddy MCS, Rao VV. Experimental studies on thermal conductivity of blends of ethylene glycol–water-based TiO_2 nanofluids. Int Commun Heat Mass Transf. 2013;46:31–6.
29. Sundar LS, Farooky MH, Sarada SN, Singh MK, Farooky H, Sarada SN, et al. Experimental thermal conductivity of ethylene glycol and water mixture based low volume concentration of Al_2O_3 and CuO nanofluids. Int Commun Heat Mass Transf. 2013;41:41–6.

30. Sundar LS, Ramana EV, Singh MK, Sousa ACM. Thermal conductivity and viscosity of stabilized ethylene glycol and water mixture Al_2O_3 nano fluids for heat transfer applications: an experimental study. Int Commun Heat Mass Transf. 2014;56:86–95.
31. Serebryakova MA, Dimov SV, Bardakhanov SP, Novopashin SA. Thermal conductivity, viscosity and rheology of a suspension based on Al_2O_3 nanoparticles and mixture of 90% ethylene glycol and 10% water. Int J Heat Mass Transf. 2015;83:187–91.
32. Guo Y, Zhang T, Zhang D, Wang Q. Experimental investigation of thermal and electrical conductivity of silicon oxide nanofluids in ethylene glycol/water mixture. Int J Heat Mass Transf. 2018;117:280–6.
33. Elias MM, Mahbubul IM, Saidur R, Sohel MR, Shahrul IM, Khaleduzzaman SS, et al. Experimental investigation on the thermo-physical properties of Al_2O_3 nanoparticles suspended in car radiator coolant. Int Commun Heat Mass Transf. 2014;54:48–53.
34. Hamid KA, Azmi WH, Mamat R, Usri NA. Thermal conductivity enhancement of TiO_2 nanofluid in water and ethylene glycol (EG) mixture. Indian J Pure Appl Phys. 2016;54:651–5.
35. Chiam HW, Azmi WH, Usri NA, Mamat R, Adam NM. Thermal conductivity and viscosity of Al_2O_3 nanofluids for different based ratio of water and ethylene glycol mixture. Exp Therm Fluid Sci. 2017;81:420–9.
36. Krishnakumar TS, Sheeba A, Mahesh V, Prakash MJ, Jose Prakash M. Heat transfer studies on ethylene glycol/water nanofluid containing TiO_2 nanoparticles. Int J Refrig. 2019;102:55–61.
37. Maxwell JC. Electricity and magnetism. Oxford: Clarendon; 1873.
38. Hamilton RL, Crosser OK. Thermal Conductivity of heterogeneous two-component systems. In: Industrial & engineering chemistry fundamentals, vol. 1. American Chemical Society; 1962. p. 187–91.
39. Lu S-Y, Lin H. Effective conductivity of composites containing aligned spheroidal inclusions of finite conductivity. J Appl Phys. 1996;79:6761–9.
40. Bhattacharya P, Saha SK, Yadav A, Phelan PE, Prasher RS. Brownian dynamics simulation to determine the effective thermal conductivity of nanofluids. J Appl Phys. 2004;95:6492–4.
41. Hojjat M, Etemad SG, Bagheri R, Thibault J. Thermal conductivity of non-Newtonian nanofluids: experimental data and modeling using neural network. Int J Heat Mass Transf. 2011;54:1017–23.
42. Ariana MA, Vaferi B, Karimi G. Prediction of thermal conductivity of alumina water-based nanofluids by artificial neural networks. Powder Technol. 2015;278:1–10.
43. Hemmat Esfe M, Afrand M, Yan WM, Akbari M. Applicability of artificial neural network and nonlinear regression to predict thermal conductivity modeling of Al_2O_3–water nanofluids using experimental data. Int Commun Heat Mass Transf. 2015;66:246–9.
44. Hemmat Esfe M, Rostamian H, Afrand M, Karimipour A, Hassani M. Modeling and estimation of thermal conductivity of MgO–water/EG (60:40) by artificial neural network and correlation. Int Commun Heat Mass Transf. 2015;68:98–103.
45. Tahani M, Vakili M, Khosrojerdi S. Experimental evaluation and ANN modeling of thermal conductivity of graphene oxide nanoplatelets/deionized water nanofluid. Int Commun Heat Mass Transf. 2016;76:358–65.
46. Ahmadloo E, Azizi S. Prediction of thermal conductivity of various nanofluids using artificial neural network. Int Commun Heat Mass Transf. 2016;74:69–75.
47. Wang X, Yan X, Gao N, Chen G. Prediction of thermal conductivity of various nanofluids with ethylene glycol using artificial neural network. J Therm Sci. 2019;1–9.
48. Hemmat Esfe M, Saedodin S, Bahiraei M, Toghraie D, Mahian O, Wongwises S. Thermal conductivity modeling of MgO/EG nanofluids using experimental data and artificial neural network. J Therm Anal Calorim. 2014;118:287–94.
49. Zhao N, Li Z. Experiment and artificial neural network prediction of thermal conductivity and viscosity for alumina–water nanofluids. Materials. 2017;10:552.
50. Hemmat Esfe M. Designing an artificial neural network using radial basis function (RBF-ANN) to model thermal conductivity of ethylene glycol–water-based TiO2 nanofluids. J Therm Anal Calorim. 2017;127:2125–31.
51. ASHRAE. Handbook—Fundamentals (SI Edition), American Society of Heating, Refrigerating and Air-Conditioning Engineers, Inc. 2017.
52. Yang L, Mao M, Huang J, Ji W. Enhancing the thermal conductivity of SAE 50 engine oil by adding zinc oxide nano-powder: an experimental study. Powder Technol. 2019;356:335–41.
53. Yang L, Ji W, Zhang Z, Jin X. Thermal conductivity enhancement of water by adding graphene nano-sheets: consideration of particle loading and temperature effects. Int Commun Heat Mass Transf. 2019;109:104353.
54. Yang L, Ji W, Huang J, Xu G. An updated review on the influential parameters on thermal conductivity of nano-fluids. J Mol Liq. 2019;296:111780.
55. Gangadevi R, Vinayagam BK, Senthilraja S. Effects of sonication time and temperature on thermal conductivity of CuO/water and Al_2O_3/water nanofluids with and without surfactant. Mater Today Proc. 2018;5:9004–11.